CO_2-Assisted Polymer Processing: A New Alternative for Intractable Polymers

Manuel Garcia-Leiner, Alan J. Lesser

Polymer Science and Engineering Department, University of Massachusetts, Amherst, Massachusetts 01003

Received 20 November 2003; accepted 3 March 2004
DOI 10.1002/app.20619
Published online in Wiley InterScience (www.interscience.wiley.com).

ABSTRACT: CO_2-assisted polymer processing is proposed as an alternative route for intractable and high molecular weight polymers based on the plasticization effects of CO_2 and its direct effect on the melting behavior of semicrystalline polymers. A modified processing system was used to process a variety of polymers in the presence of high-pressure CO_2. The system includes an extruder that was modified to allow for high pressures created by the injection of CO_2. The new design includes a modified feed section that allows a given mass of polymer to interact with CO_2 before and during the extrusion process. The inherent shear mixing and the presence of CO_2 allow for a specific control over the extrudate morphology. Results suggest that this alternative design provides a new and easy route to melt process high melt viscosity polymers of commercial importance, such as polytetrafluoroethylene (PTFE), fluorinated ethylene propylene copolymer (FEP), and syndiotactic polystyrene (s-PS). The increased processability of these systems in CO_2 is related to the plasticization effect of CO_2 that was quantified through a depression in the glass-transition temperature according to the Chow model. J Appl Polym Sci 93: 1501–1511, 2004

Key words: processing; supercritical carbon dioxide; fluoropolymers; syndiotactic polystyrene; extrusion

INTRODUCTION

The idea of using CO_2 particularly at supercritical conditions as an alternative processing aid in polymer extrusion has been analyzed extensively for the past two decades.[1–13] The interest in supercritical CO_2 ($scCO_2$) is a natural consequence of the fact that its inherent properties are very close to those required in a successful blowing agent. At supercritical conditions, CO_2 combines in a unique manner, properties from both liquid and gas states, exhibiting liquidlike densities along with low viscosities and high diffusion rates that are typical of a gas phase.[14–21] In addition, the low toxicity and flammability, together with the reduced cost of CO_2, make it a real and environmentally friendly alternative for polymer processing. Because of its high compressibility, the solvent/plasticizer properties of CO_2 can be tuned and controlled by small changes in temperature and pressure, acting as a "reversible plasticizer" that can be easily removed from the system during depressurization. During extrusion, CO_2 dissolves into a molten polymer under moderately high pressures, and diffuse away from the polymer substrate at ambient conditions, leaving the final product solvent-free, thus reducing the costs of solvent removal.[22]

A vast amount of research, particularly in the area of polymeric foams, has been focused in studying the relation between the processing conditions in extrusion and the final polymer morphology when CO_2 is introduced.[1–13] The initial concentration, solubility, and diffusivity of the gas in the polymer melt all have a direct effect on the final properties of the foam.

In this work, CO_2-assisted polymer processing was used for a variety of polymers at conditions very close to or in the supercritical regime for CO_2. The results suggest that the alternative design of the system facilitates the melt processing of intractable polymers of commercial importance such as polytetrafluoroethylene (PTFE), fluorinated ethylene propylene copolymer (FEP), and syndiotactic polystyrene (s-PS). Polymeric foams, down to the microcellular range, were obtained in some cases and a good understanding of the relation between the processing conditions and the final extrudate morphology was obtained, suggesting that the plasticization process of CO_2 governs the processability of these materials, thus providing a new and easy route to melt process high melt viscosity polymers. The description of the plasticization phenomenon, provided by Chow's model, through an estimation of the glass-transition depression in these systems was used to correlate our experimental observations.

Correspondence to: A. Lesser (ajl@mail.pse.umass.edu).
Contract grant sponsor: Materials Research Science and Engineering Center (MRSEC), University of Massachusetts (UMASS).
Contract grant sponsor: Center for UMASS/Industry Research on Polymers (CUMIRP)—Cluster G.

EXPERIMENTAL

A single-screw extruder (RCP-025 Microtruder, Randcastle Extrusion Systems, Cedar Grove, NJ) with a working L/D ratio of 24 and a screw diameter of 6.35 mm (1/4 in.) was used to process a variety of polymers. The extrusion system, as depicted in Figure 1, has a vertical feeding with the screw driven through the metering section and no additional mixing devices. Temperature was controlled through four independent heaters located in the die and along the extruder barrel. A 1-mm tubular die was used along with a take-up roller for the spinning of the final extrudate. The feed section in the extruder was modified to allow for the high pressures promoted by the injection of CO_2. The new feed section, constructed primarily of standard high-pressure fittings, included a modified hopper that allows a specific amount of polymer to interact with CO_2 before the extrusion process. The conditions inside the hopper were precisely controlled: temperature was manipulated using a temperature controller and a pressure gauge directly attached to the feed section was used to monitor the internal pressure. CO_2 was injected using a high-pressure carbon dioxide pump (Hydro-Pac, Inc., Fairview, PA) with a maximum discharge pressure of 286.84 MPa.

Differential scanning calorimetry (DSC) was used to study the thermal behavior of the polymers processed in our system. DSC experiments were carried out in a thermal analyst model 2910 DSC (TA Instruments, New Castle, DE), at relatively slow heating rates (1–10°C/min), to obtain a quantitative response of the thermal properties of each sample. The crystallinity of the samples was estimated by the ratio of their melting enthalpy and the theoretical heat of fusion for a perfect crystal of the corresponding polymer.

The overall extrudate morphology obtained at different processing conditions was investigated using scanning electron microscopy (SEM). Samples were cryofractured in liquid nitrogen and gold coated before the SEM analysis. SEM images were obtained using a field emission scanning electron microscope (FESEM; JSM-6320FXV; JEOL, Peabody, MA) and a SEM model JEOL-CF-35 with a filament voltage of 20,000 V.

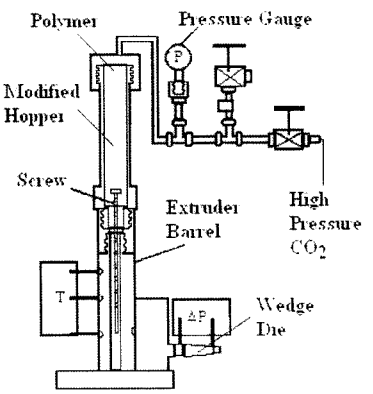

Figure 1 Modified extrusion system for CO_2-assisted polymer processing.

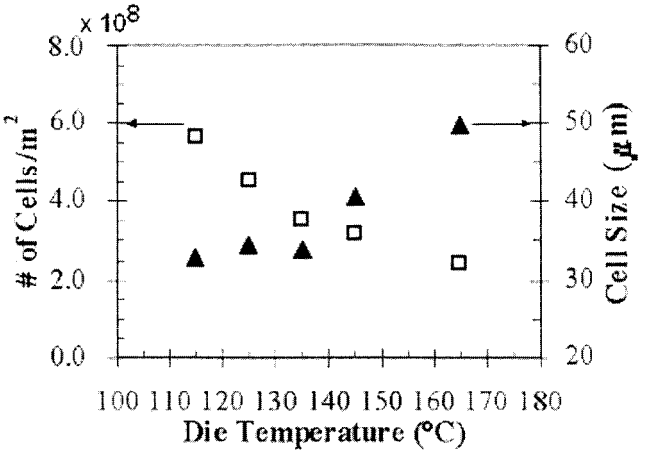

Figure 2 Influence of die temperature on the overall morphology of HDPE extrudates processed at 190°C (saturation time = 140 min; pressure = 5.86 MPa).

RESULTS AND DISCUSSION

CO_2-assisted polymer processing and plasticization

A specific control over the final extrudate morphology was obtained using the modified processing system described before. Initial results using high-density polyethylene (HDPE) showed that both the presence of CO_2 in the feed section and the diffusion rate of CO_2 in the polymer melt promote the appearance of a foamed structure. If the material is saturated in CO_2 for a given time, cell nucleation may be observed, even at moderate pressures (3.44 MPa), which suggests that the diffusion rate of CO_2 into the melt controls the nucleation process. With a saturation time, the dissolution of CO_2 in the melt increases, and nucleation is dictated only by the processing conditions. When a favorable nucleation process is observed, specific control on the morphology can be achieved by altering several parameters in the system, such as the temperature distribution and the saturation pressure.[23] An example is shown in Figure 2, where by changing the temperature distribution in the system the nucleation process is controlled, and polymer foams with different cell density (number of cells per unit area) and cell size are produced. As shown in this figure, the polymer can be continuously processed at temperatures even below its melting point (127°C for HDPE) when CO_2 is introduced into the system, suggesting a significant amount of plasticization brought about by the presence of CO_2. These results suggest that the alter-

native design of the system allows not only for a specific control of the morphology of the extrudate, but also provides a direct way to estimate the amount of plasticization in the system imposed by CO_2 under certain conditions.

To quantify the plasticization effect of CO_2 in a given polymer we used the model proposed by Chow[25] that describes the plasticization phenomenon using a molecular interpretation of the glass-transition temperature of polymer–diluent systems. Plasticization is described in terms of the glass-transition depression that occurs in a polymer–diluent system resulting from the presence of a small-molecule diluent, such as CO_2, at low concentrations. The model provides an explicit expression for the glass-transition depression (T_g/T_{g0}) as the ratio of the glass-transition temperature of a polymer–diluent system (T_g) to that of the pure polymer (T_{g0}), using an equilibrium approach in terms of the change in configurational entropy of a system during the glass formation.

On the basis of both classical and statistical thermodynamics, Chow proposed the following expression to describe the glass-transition depression:

$$\ln\left(\frac{T_g}{T_{g0}}\right) = -\frac{1}{\Delta C_p}\left[\ln\left(\frac{Q^N_{\text{liquid}}}{Q^0_{\text{liquid}}}\right) + T\frac{\partial}{\partial T}\ln\left(\frac{Q^N_{\text{liquid}}}{Q^0_{\text{liquid}}}\right)\right] \quad (1)$$

where ΔC_p is the difference in heat capacity at constant pressure between the supercooled liquid and glass, and Q is the configurational partition function of the system. Using the Bragg–Williams approximation of an order–disorder transition to determine the configurational partition function, the model suggests that in the plasticization of a polymer by a small molecule diluent such as CO_2, the main contribution to the partition function—and so to the ratio T_g/T_{g0}—comes from the mixing of diluent molecules among lattice sites, and thus the main interest relies on the configurations of small molecules on the lattice rather than on the arrangement of the polymer itself (given that T_{g0} is known). Using this approximation, the partition function of the pure polymer is always equal to unity and that of a polymer–diluent system is given in terms of the energetic interactions of the diluent molecules:

$$Q^N_{\text{liquid}} = \frac{(N+L)!}{N!L!}\exp\left(\frac{NL}{N+L}\frac{z\varepsilon}{2kT}\right) \quad (2)$$

where N is the number of diluent molecules randomly distributed in a lattice of $N + L$ sites, L is the number of vacant sites, and z is the lattice coordination number that can be roughly estimated by the nearest whole number to the ratio of the molecular weights of the monomer and diluent.[26] Also, $\epsilon = \epsilon_{NN} + \epsilon_{LL} - 2\epsilon_{NL}$, with ϵ_{NN}, ϵ_{LL}, and ϵ_{NL} describing the energies of each *NN*, *LL*, and *NL* pair, respectively. By substituting, the final expression for the Chow model is obtained as

$$\ln\left(\frac{T_g}{T_{g0}}\right) = \beta[(1-\theta)\ln(1-\theta) + \theta\ln\theta] \quad (3)$$

where β and θ are nondimensional parameters, given by

$$\beta = \frac{zR}{M_p\Delta C_{pp}} \quad (4)$$

$$\theta = \frac{N}{N+L} = \frac{M_p}{2M_d}\frac{\omega}{1-\omega} = \frac{V_p}{2V_d}\frac{\phi}{1-\phi} \quad (5)$$

where M_p and M_d are the molecular weights of the polymer repeating unit and diluent, respectively; ΔC_{pp} is the excess transition isobaric specific heat of the polymer; ω and ϕ represent the weight and volume fraction of diluent in the system, respectively; and V_p and V_d correspond to the molar volumes of the polymer repeating unit and diluent, respectively.

Equation (3) provides an explicit expression to quantify the plasticization process of a polymer–diluent system in terms of intrinsic properties of the pure polymer and diluent. In our system, this expression can be used to quantify the amount of plasticization, using only two parameters that are either available in the literature or that can be easily estimated or prescribed by the processing conditions. It is easy to recognize that β is dependent only on the magnitude of ΔC_{pp}, a thermodynamic property of the polymer. On the other hand, θ depends on the weight fraction of CO_2 and, because the conditions at the hopper can be specifically controlled, the value of θ can be prescribed for each polymer system, setting the system to equilibrium conditions, where the concentration of CO_2 is dictated by the equilibrium mass uptake of the polymer, as determined in conventional diffusion experiments.

Figure 3 shows the predictions of the Chow model, as described in eqs. (3)–(5), to the plasticization process of HDPE by CO_2. The parameters[27] and results obtained in this case are also summarized in Table I. The Chow model suggests the existence of a region in which the glass transition of the system is substantially affected by the presence of CO_2. The limit of this region is obviously dictated by the amount of CO_2 that can be introduced into the polymer at equilibrium conditions. As shown in this figure, despite the fact that the equilibrium mass uptake of CO_2 is rather small (6%), the glass-transition depression is considerable and the ratio T_g/T_{g0} decreases to 0.8730. This value corresponds to an absolute change in glass transition of 30.09°C, thus reducing the overall T_g of the system to 206.91 K. These calculations correlate very

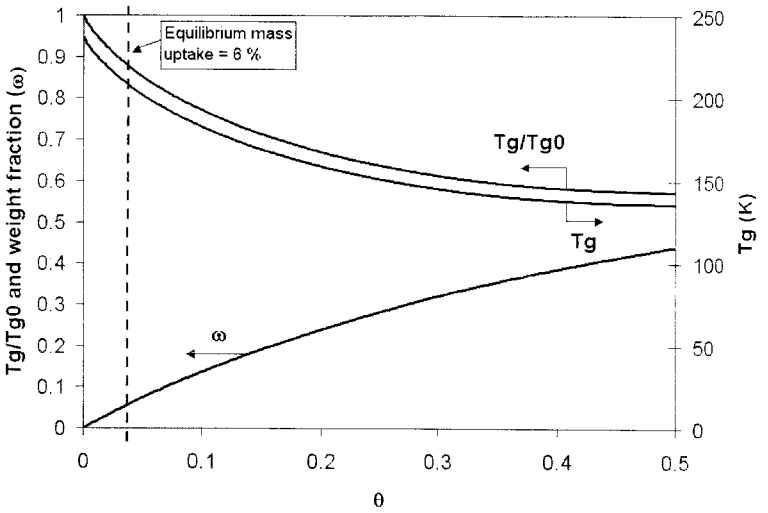

Figure 3 Glass-transition depression (T_g/T_{g0}) for the polyethylene–CO_2 system, as predicted by the Chow model. The dashed line indicates the equilibrium mass uptake of CO_2 for the case of polyethylene (6%). Note that the relation between the weight fraction of CO_2 (ω) and the parameter θ is not linear.

well with the experimental observations made earlier for HDPE, suggesting a significant amount of plasticization promoted by introducing CO_2 that enhances the processability of HDPE at lower temperatures (even below the melting point).

These results suggest that the presence of CO_2 not only controls the final morphology, but it also facilitates the polymer processing through a combination of both plasticization and the imposed hydrostatic pressure acting as a processing aid during extrusion. This is a distinctive feature of our system, which enables the processing of high melt viscosity or intractable polymers, something impossible to achieve in a conventional extruder. Results obtained for syndiotactic polystyrene (s-PS), fluorinated ethylene propylene copolymer (FEP), and polytetrafluoroethylene (PTFE) using this alternative processing route are discussed below.

Processing of intractable polymers

Polytetrafluoroethylene (PTFE)

Because of their high service temperatures and chemical inertness, fluoropolymers are a very attractive group of materials for CO_2-assisted polymer processing. In particular, PTFE might be a good candidate for this alternative processing method because of its well-known affinity to CO_2. In general PTFE shows an extremely high molecular weight, resulting in a melt viscosity that is about 6 orders of magnitude higher than that of most common thermoplastic polymers (10^{10}–10^{12} Pa · s). The chemical inertness and stability as well as the low surface energy of PTFE are provided by its helical conformation, which creates an almost perfect cylindrical structure that consists of an outer layer of fluorine atoms surrounding a carbon-based core.[24] As a consequence, the processing alternatives

TABLE I
Material Properties, Parameters, and Results Obtained with the Chow Model

	Polymer			
Parameter	Polyethylene	PTFE	FEP	Polystyrene
T_{g0} (K)	237	200	180	358.5
ΔC_{pp} (J g^{-1} K^{-1})	0.3708	0.0939	0.1361	0.2592
M_p (g mol^{-1})	28.04	100.02	106.52	104.15
M_d (g mol^{-1})	44.09	44.09	44.09	44.09
M_p/M_d	0.636	2.268	2.416	2.362
z	1	2	2	2
$M_p\Delta C_{pp}$ (J mol^{-1} K^{-1})	10.4	9.4	14.75	27
Equilibrium mass uptake of CO_2 (%)	6	3.5	4.4	11.8
ΔT_g (K)	30.09	52.41	38.74	84.54
T_g (K)	206.91	147.59	141.26	273.96
T_g/T_{g0}	0.8730	0.7379	0.7847	0.7641

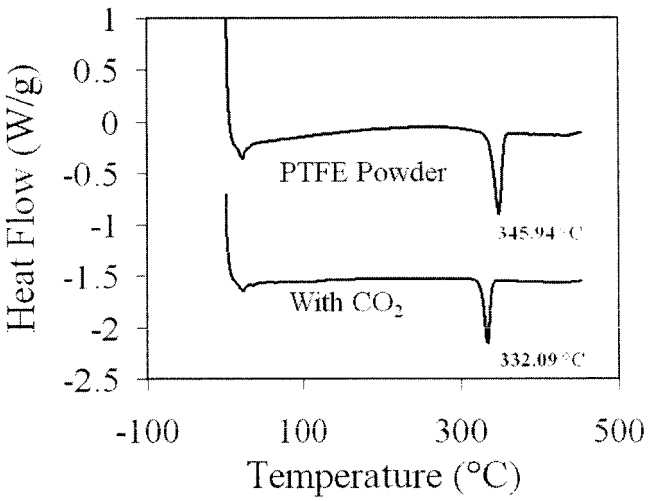

Figure 4 Typical thermal behavior of PTFE samples processed in our system at 360°C.

for PTFE are reduced to RAM extrusion and compression molding, and the possibility of an alternative and easy processing route for PTFE is of major relevance.

PTFE powder (particle size = 35 μm) was processed in our system in the presence of CO_2. Results suggest that, despite the extremely high molecular weight of PTFE, a continuous processing is obtained when CO_2 was introduced, significantly enhancing the processability of PTFE in the presence of CO_2. The thermal behavior of the samples obtained with CO_2 is presented in Figure 4. As typically observed, the virgin polymer has a melting point of 345.94°C, with a corresponding degree of crystallinity of 62.4%, using a value of 102.1 J/g as the enthalpy of fusion for 100% crystalline PTFE.[28] In contrast, the melt-processed sample displays a lower degree of crystallinity (25.9%) and a significantly lower melting temperature (327.88°C). This dramatic change in the thermal response is evidence of the melting process of the sample during extrusion. After melting, the recrystallization process is restricted because of the extremely high melt viscosity and, as a consequence, the crystallinity of the sample is significantly reduced. In this particular case, the melt viscosity is so high that, upon melting, more than 50% of the crystallinity is lost. The restricted recrystallization process significantly reduces the typical crystal size, and thus the lower melting point.

A typical example of the final morphology observed in the PTFE extrudates is presented in Figure 5. Well-defined foamed structures with enough cell integrity, even at such high temperatures, are obtained. This figure shows a SEM image of a PTFE sample obtained at 360°C: in this particular case, the average cell size is below 10 μm, a cell size typically observed in microcellular materials. As in the case of HDPE, the final morphology can be specifically controlled through the processing conditions, so that a decrease in the die temperature allows for a specific control on the average cell size and cell density. The saturation pressure can also be used to control the general morphology. At higher pressures, especially above the critical point, both density and concentration of CO_2 are increased and, consequently, the nucleation process is enhanced.[23] However, as mentioned before, our design allows for a given saturation time in CO_2 before processing that promotes cell nucleation, even at moderate pressures (3.44 MPa), which suggests that even in the case of PTFE, the nucleation process can be tuned so that a specific control over the cell density and cell size can be obtained.

The high melt viscosity does not limit the processability of PTFE by this route, and a continuous process is observed even at temperatures below the polymer melting point (285°C), suggesting a significant amount of plasticization by CO_2. Figure 6 shows the predictions of the Chow model for the plasticization process of PTFE by CO_2. The parameters used in this calculation are summarized in Table I and include a value of 3.5% for the equilibrium mass uptake of CO_2 for PTFE[28] and a change in heat capacity during glass transition ($M_p\Delta C_{pp}$) of 9.4 J mol^{-1} K^{-1}.[29,30] The model predicts the existence of a large plasticizing region that extends until the equilibrium mass uptake of CO_2 is reached, and again, despite the fact that this value is very low (3.5%), the glass transition of the system is significantly affected by CO_2, decreasing the magnitude of the ratio T_g/T_{g0} to 0.7379. This result corresponds to an almost 30% decrease in the T_g of the system, displaying an absolute change in glass transition of 52.41°C and thus reducing the overall T_g of the system to 147.59 K. Once again, these calculations indicate that the plasticization process promoted by CO_2 is large enough to allow for a continuous processing of PTFE at lower temperatures using this alternative processing strategy.

Fluorinated ethylene propylene copolymer (FEP)

FEP, which can also be successfully processed in our system, is a random copolymer of tetrafluoroethylene

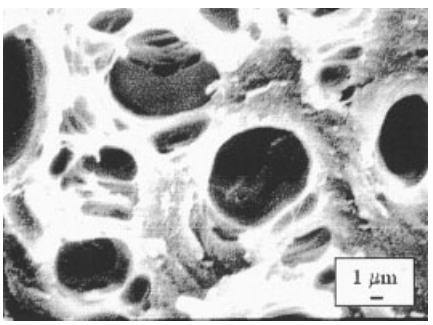

Figure 5 Overall morphology observed in PTFE samples processed at 360°C.

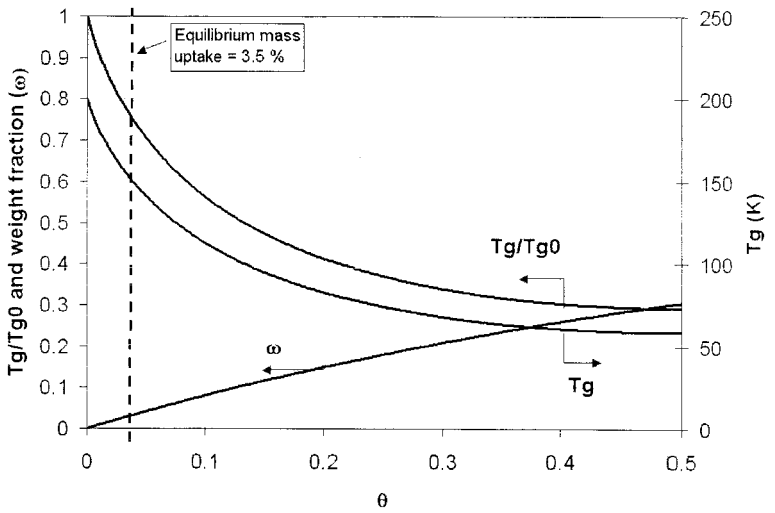

Figure 6 Glass-transition depression (T_g/T_{g0}) for the PTFE–CO_2 system, as predicted by the Chow model. The dashed line indicates the equilibrium mass uptake of CO_2 for the case of PTFE (3.5%).

(TFE) and hexafluoropropylene (HFP), with a structure very similar to that of PTFE except for the HFP units that are responsible for significant changes in the physical properties of the system, acting as defects in crystallites that reduce the overall melting point to 260°C.[24] As a consequence, FEP has a reduced melt viscosity, compared to that of PTFE, that enhances its processability.

The thermal behavior of the FEP samples (13% HFP) processed in our system is presented in Figure 7. As shown in this figure, despite the similarity with PTFE, significant differences are observed in the general behavior of both polymer systems. The thermal behavior of the FEP samples appears to be independent of the processing conditions, such that the DSC traces of these materials are very similar, regardless of the presence of CO_2. In addition, the thermal behavior of the melt-processed samples is almost identical of that observed in the virgin powder. The crystallinity of the virgin polymer in this case is around 41.38%, using 92.94 J/g as the enthalpy of fusion for 100% crystalline FEP.[31] This value is very similar to that observed in the samples processed with and without CO_2 (40.37 and 37.0%, respectively), and it appears not to be affected in a significant way by the melting process. This general behavior is a consequence of the inherently larger processability of FEP that, despite the high molecular weight, does not restrict the recrystallization process, so that most of the crystallinity in the sample can be recovered after melting.

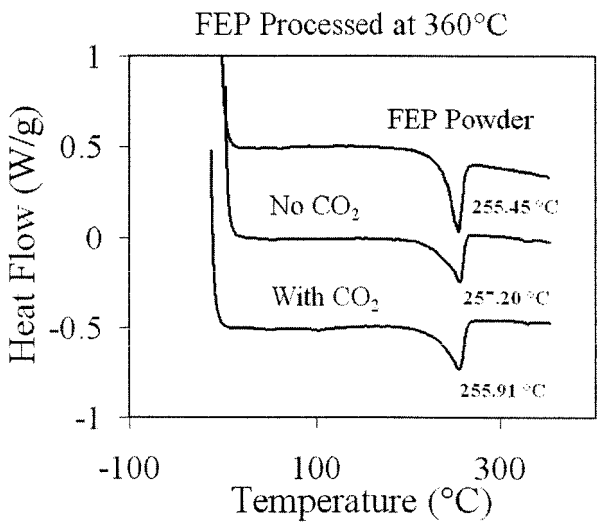

Figure 7 Typical thermal behavior of FEP samples processed in our system at 360°C.

The enhanced processability of FEP significantly facilitates the specific control of the morphology of the FEP extrudates when CO_2 is introduced. In this case, despite the high temperatures, the nucleation process can be enhanced by lowering the die temperature, thus promoting an increase in the cell density and decreasing the cell size. At high temperatures (360°C) the foamed structure is evident, although a significant amount of cell coalescence is present; however, at lower temperatures (285°C) the cell structure is better defined and the integrity of the cells increases, as shown in Figure 8. At these temperatures, a well-defined closed-cell structure is observed and the typical average cell size is around 10 μm. Regarding the nucleation process, it is expected that without a foaming agent, as in this case, homogeneous nucleation dominates and nucleation is promoted by a thermodynamic instability in the process, which is typically obtained by the decrease in pressure along the extrusion line.[4] The homogeneous process, characterized by a typical thermodynamic barrier related to the energy

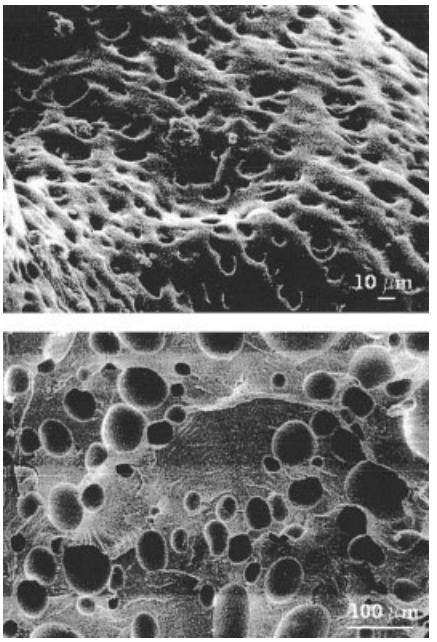

Figure 8 Typical closed-cell morphology obtained in FEP at 285°C.

needed to create a nucleus, is responsible for the majority of the voids in the sample. However, in the presence of small impurities, a thermodynamically more favorable heterogeneous nucleation mechanism occurs, which in addition to cell coalescence promotes the appearance of large cells in the sample.

Once again, a continuous process is obtained in FEP samples; however, in this case the high melt viscosity restricts the processability of FEP to temperatures above 285°C, regardless of the presence of CO_2. This observation suggests that the plasticization process in this case is not as important as in the case of PTFE, so that the glass-transition depression observed in FEP, attributed to the presence of CO_2, should be lower that that of PTFE at equilibrium conditions.

The plasticization process of FEP by CO_2 can also be described by the Chow model. In this case, however, no available data were found in the literature regarding the heat capacity change of FEP at the glass transition (ΔC_{pp}). Using the additivity concept of the heat capacities of linear polymers proposed by Gaur and Wunderlich[32,33] a change in heat capacity during glass transition ($M_p \Delta C_{pp}$) can be estimated. This calculation is based on the fact that, because the concentration of HFP units in the copolymer is known, their contribution to the heat capacity can be estimated. According to this theory, a dimer containing one unit of HFP attached to one of TFE creates a four-bead structure with a corresponding $M_p \Delta C_{pp}$ of 45.2 J mol^{-1} K^{-1}. In contrast, a one-bead structure is created when two TFE units are attached to each other. In this case, the structure is identical to that of a PTFE dimer and so the corresponding $M_p \Delta C_{pp}$ is 9.4 J mol^{-1} K^{-1}. Given the concentration of HFP units in the copolymer (13%), a value of 14.75 J mol^{-1} K^{-1} is estimated.

Figure 9 shows the results obtained using the parameters in Table I. The predictions correlate very well with the experimental observations, showing the existence of a large plasticizing region limited by the equilibrium mass uptake of CO_2 (4.4%). The important observation here is that, despite the fact that this value is larger than that observed in PTFE (3.5%), the model predicts that at equilibrium conditions, the value of the glass-transition depression ratio T_g/T_{g0} is 0.7847, which corresponds to an absolute change in glass transition of 38.71°C, less than that observed in PTFE. These results indicate that, even though the plasticization process of FEP by CO_2 is large, it is less impor-

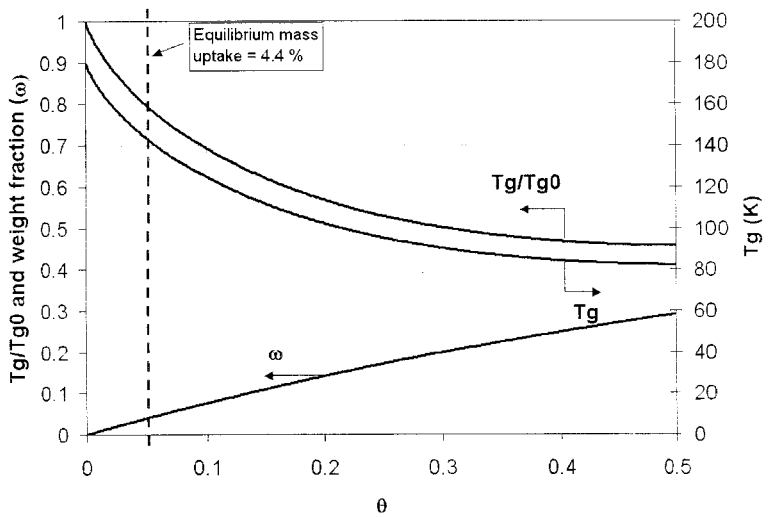

Figure 9 Glass-transition depression (T_g/T_{g0}) for the FEP–CO_2 system, as predicted by the Chow model. The dashed line indicates the equilibrium mass uptake of CO_2 for the case of FEP (4.4%).

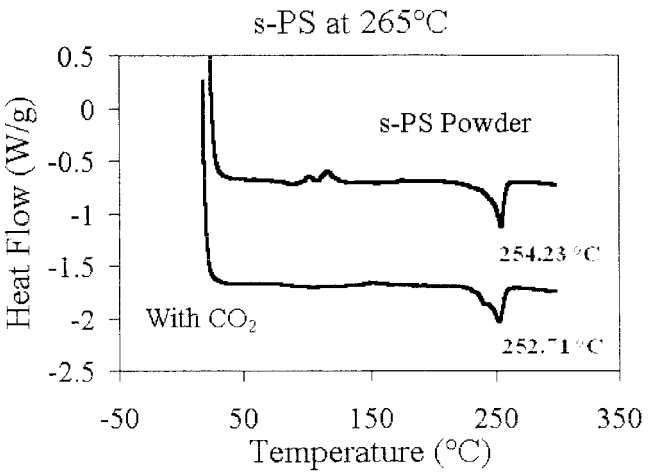

Figure 10 Typical thermal behavior of s-PS samples processed in our system at 265°C.

tant than that observed in PTFE and, because of the high melt viscosity of the system, it is not sufficient to allow for a continuous processing at temperatures close to the melting point.

Syndiotactic polystyrene (s-PS)

In addition to fluoropolymers, high melt viscosity polyolefins are also good candidates to be processed using this route. An example of these materials is s-PS, which is a relatively new partially crystalline commodity plastic with a high melting point (>250°C), suggesting higher service temperatures than those of common plastics. The relevance of s-PS as an engineering polymer is that the amount of crystallinity, the type of crystal structure, and morphology can be controlled by the crystallization conditions. Thus, a consistent strategy for melt process s-PS is of great relevance, given that the properties that make s-PS an attractive material (high-temperature mechanical properties, low permeability, good chemical resistance) are strongly affected by the amount and distribution of the crystalline phase.

Figure 10 describes the typical thermal behavior of the s-PS samples processed in our system. As in the case of FEP, the thermal behavior appears to be independent of the processing conditions, and so the DSC trace of a sample processed with CO_2 differs slightly from that of the s-PS virgin powder used. However, because of the lack of additional mixing devices in the extruder, processing without the addition of CO_2, it is almost impossible because of the high molecular weight, so a comparison between samples processed with and without CO_2 cannot be achieved in this case. The crystallinity of the virgin polymer in this case is 47.76%, using 53.2 J/g as the enthalpy of fusion of 100% crystalline s-PS.[34] Again, similar to what is observed in FEP, this is very similar to the value observed in the CO_2-processed samples (48.10%), suggesting that the recrystallization process is not restricted, despite the high molecular weight, so that after melting most of the crystallinity in the sample can be recovered. In addition, as shown in Figure 10, no significant changes in the melting point are observed.

As in any other systems, the overall morphology of s-PS extrudates can be controlled by the processing conditions and, given the right conditions, a well-defined foam structure is observed, showing increases in the cell density at lower temperatures.

Despite the high melt viscosity of s-PS, a continuous process is obtained with CO_2, suggesting a considerable amount of plasticization. In this case, however, the processability is limited at temperatures very close to the melting point (255°C), at which the high melt viscosity prohibits a continuous processing. Again, this observation suggests that the plasticization process in this case is not as important as in the case of PTFE, and that the glass-transition depression observed in s-PS, attributed to the presence of CO_2, should be very similar to or slightly larger than that observed in the case of FEP.

Figure 11 shows the predictions to the plasticization process of s-PS by CO_2 using the Chow model. In this particular case, it is important to point out that, because specific details on tacticity or crystallinity are not prescribed in the model, and because no available data are found in the literature regarding the heat capacity change (ΔC_{pp}) or equilibrium mass uptake of CO_2 for s-PS, the parameters used in this figure correspond to those of amorphous polystyrene.[35,36] The predictions, however, correlate very well with the experimental observations, showing a large plasticizing region limited by the equilibrium mass uptake of CO_2 (11.8%). In this case, the T_g/T_{g0} value is 0.7641, which corresponds to a smaller change than that of PTFE. These results indicate that, even though the mass uptake of CO_2 is very large in this case, the plasticization process of s-PS by CO_2, as judged by the ratio T_g/T_{g0}, is larger than that observed in FEP but smaller than that in the case of PTFE, which correlates exactly with the observed processability of these systems.

Plasticization and the effect of CO_2 on the melting behavior of semicrystalline polymers

As described before, the Chow model appears to be appropriate for describing the plasticization process of a polymer in the presence of CO_2. The predictions of the model for the polymers used in this study are shown in Figure 12. The presence of CO_2 promotes a depression in the glass transition that is dependent on the intrinsic properties of the system. The rate of depression is very large for the case of PTFE, displaying

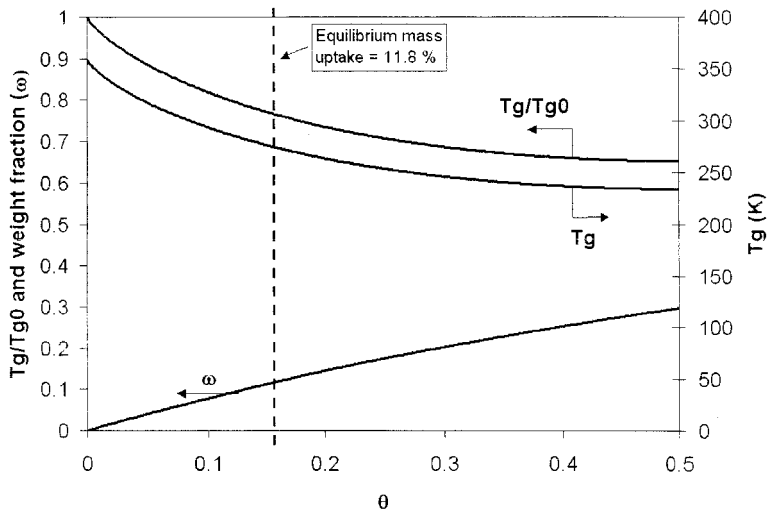

Figure 11 Glass-transition depression (T_g/T_{g0}) for the polystyrene–CO_2 system, as predicted by the Chow model. The dashed line indicates the equilibrium mass uptake of CO_2 for the case of polystyrene (11.8%).

a very pronounced slope, whereas the lowest rate of depression is observed in s-PS. In contrast, the largest equilibrium mass uptake of CO_2 is observed in s-PS (11.8%), whereas the smallest value corresponds to PTFE. In this regard, it appears that the overall plasticization process is dictated by a combination of the rate of depression in the glass transition and the equilibrium mass uptake of CO_2 for a given polymer. As proposed in the Chow model, the plasticization process can be quantified by the ratio T_g/T_{g0}, which appears to correlate well with the experimental observations. As presented in Figure 13, the processability of these systems is directly related to the magnitude of T_g/T_{g0}, suggesting that the amount of CO_2 plasticization in PTFE is larger than that observed in any of the systems studied here, and thus its increased processability at lower temperatures.

Although the plasticization effect of CO_2 in a variety of polymers has been reported extensively in the literature, the effects of CO_2 on the crystallization and melting temperatures have been analyzed for only a few systems.[36,37] In general, the behavior of the crystallization temperature (T_c) is consistent with that observed for T_g, showing a linear decrease with an increase of CO_2 pressure. However, for the specific case of s-PS, Zhang and Handa[37] showed that CO_2 promotes crystallization of glassy s-PS into its various crystalline forms (α and β) as well as to induce crystal–crystal transformations between them at a temperature below the melting temperature of the α-form.

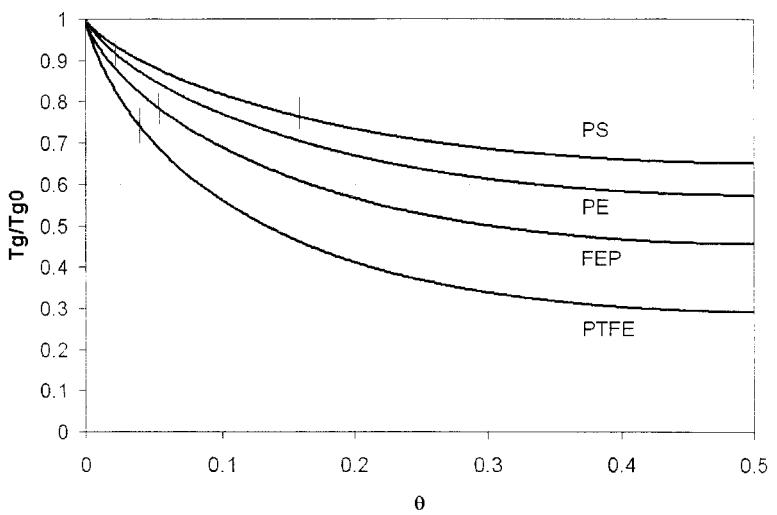

Figure 12 Chow model predictions of the glass-transition depression (T_g/T_{g0}) for the polymers used in this study. The marks indicate the equilibrium mass uptake of CO_2 for the corresponding polymer.

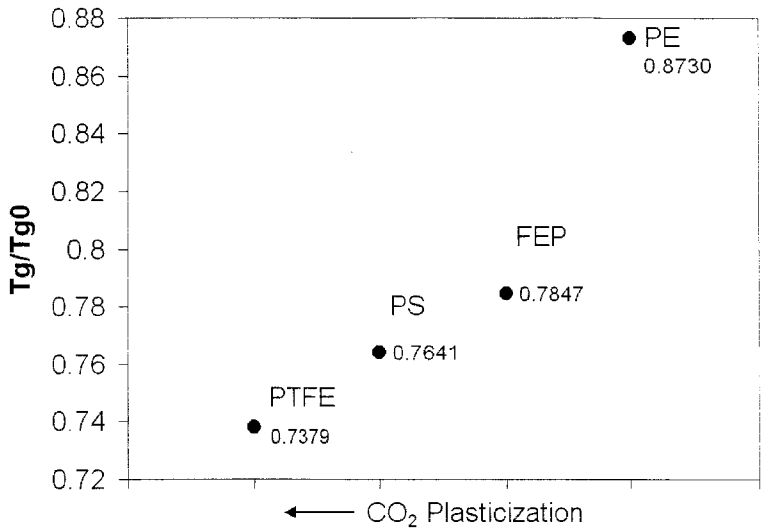

Figure 13 Plasticization process of CO_2 for the polymers used in this study, as estimated by the Chow model. As shown, the experimental observations suggest a direct relation between the glass-transition depression (T_g/T_{g0}) and the processability of these systems in CO_2.

These transitions could be understood only if the α-crystals undergo melting at a depressed temperature before transforming into the β-form. We also reported[18] crystal–crystal transformations in high-modulus, ultrahigh molecular weight polyethylene fibers when deformed in supercritical CO_2.

Using high-pressure DSC techniques Zhang and Handa[37] showed in fact that CO_2 has a direct effect on the melting behavior of semicrystalline polymers. A significant depression in the melting point is evident in the presence of dissolved CO_2. The melting temperature depression is dependent on the solubility of the gas, showing no change in T_m when CO_2 was replaced with N_2. A rapid decrease in T_m is observed initially by increasing the pressure of CO_2 until the hydrostatic contribution of CO_2 dominates, making the change in T_m smaller at elevated temperatures. The same behavior is observed in poly(ethylene terephthalate) samples, showing that the depression in melting temperature is dictated by both the polymer–gas interactions and the intrinsic crystal characteristics. These authors relate the decrease in T_m to an increase in the specific surface free energy δe caused by the dissolved CO_2. By use of the Thomson–Gibbs equation, the change in melting temperature is given by

$$T_m = T^{\circ}_{(m)}\left(1 - \frac{2\delta e}{l\Delta h}\right) \tag{6}$$

where T°_m is the melting point of an infinitely large crystal, l is the lamellar thickness, and Δh is the heat of fusion per unit volume. Because T_m, l, and Δh are generally constant, the change in T_m is attributed to δe.

This behavior is also expected to occur in other polymer–gas systems whenever the gas sorption and the plasticization effect are pronounced. As discussed before, the plasticization by CO_2 is significant for the systems studied here (PTFE, FEP, and s-PS), so that a direct effect on the melting behavior of these systems is expected to occur. This effect might certainly help to explain the enhanced processability in systems such as PTFE where a continuous process is obtained even at temperatures below the typical melting point. Furthermore, as shown in Figure 14, when PTFE is saturated in CO_2 below its melting point at relatively small pressures for a certain amount of time, the resulting material displays a decreased melting point, suggesting that at these conditions there is a direct effect of

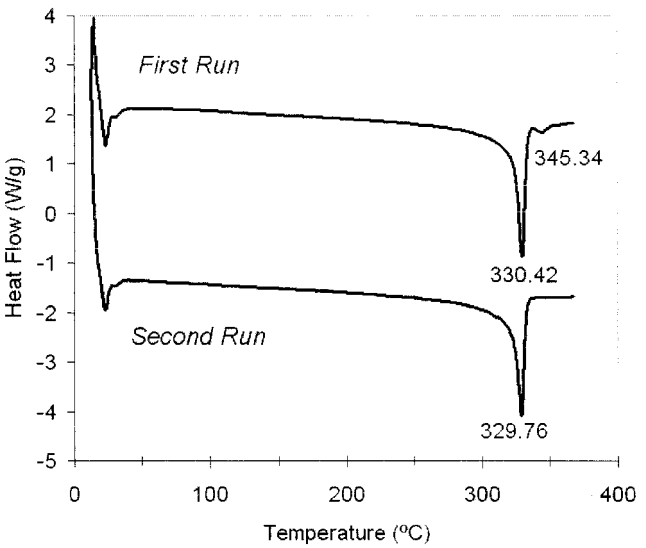

Figure 14 Thermal behavior of PTFE sample saturated in CO_2 at 330°C for 6.5 h at relatively low pressure (5.51 MPa). Shown are the first and second traces obtained in the DSC.

CO_2 on the melting behavior of PTFE. In this case, the well-known affinity to CO_2 contributes to the gas sorption, displaying a considerable plasticization effect, which, as suggested before, might be accompanied with a significant depression in the melting temperature. As mentioned before, the plasticization process appears to be smaller in the case of FEP, so that a lesser effect on the melting behavior is expected in this case, which correlates well with the lower processability of this system compared to that of PTFE and s-PS.

CONCLUSIONS

In this work, CO_2-assisted polymer processing is presented as an effective alternative to process intractable or high melt viscosity polymers. This alternative route combines both the plasticization effect and the hydrostatic contribution, brought about by the presence of CO_2, thus significantly enhancing the processability of a polymer–CO_2 system. Despite their high melt viscosity, high molecular weight, and inherent physical properties of the systems analyzed here (s-PS, FEP, and PTFE), a continuous process is obtained in CO_2 using a modified processing system. Several factors appear to have a direct effect on the final morphology of a polymer, although the diffusion rate of CO_2 in the melt appears to dominate cell nucleation by controlling the amount of gas dissolved, so that foaming is favored by a saturation time in CO_2 before extrusion.

The increased processability is directly related to the plasticization process of the polymer attributed to the presence of CO_2 and to the direct effect that dissolved CO_2 might have on the melting temperature through an increase in the specific surface free energy of the system. The amount of plasticization was quantified using the model proposed by Chow, suggesting that the improved processability of intractable materials in the presence of CO_2 can be related to the glass-transition depression ratio (T_g/T_{g0}). The plasticization process appears to be dependent on the intrinsic properties of the polymer and its interaction with CO_2, being predominantly greater for PTFE.

The authors acknowledge the Materials Research Science and Engineering Center (MRSEC) at the University of Massachusetts (UMASS) and the Center for UMASS/Industry Research on Polymers (CUMIRP)—Cluster G for their financial support for this study, and thank Dr. Bryan E. Coughlin from the Polymer Science and Engineering Department at the University of Massachusetts–Amherst for providing the s-PS samples used in this study.

References

1. Suh, N. P. In: Microcellular Plastics; Stevenson, J. F., Ed.; Innovation Polymer Process: Molding; Hanser: Munich, Germany, 1996; pp. 93–149.
2. Baldwin, D. F.; Park, C. B.; Suh, N. P. Polym Eng Sci 1996, 36, 1425.
3. Lee, S. T. J Cell Plast 2001, 37, 221.
4. Park, C. B.; Baldwin, D. F.; Suh, N. P. Polym Eng Sci 1995, 35, 432.
5. Colton, J. S.; Suh, N. P. Polym Eng Sci 1987, 27, 500.
6. Lee, M.; Tzoganakis, C.; Park, C. B. Polym Eng Sci 1998, 38, 1112.
7. Park, C. B.; Cheung, L. K. Polym Eng Sci 1997, 37, 1.
8. Colton, J. S.; Suh, N. P. Polym Eng Sci 1987, 27, 485.
9. Colton, J. S.; Suh, N. P. Polym Eng Sci 1987, 27, 493.
10. Han, C. D.; Villamizar, C. A. Polym Eng Sci 1978, 18, 687.
11. Han, C. D.; Ma, C. Y. J Appl Polym Sci 1983, 28, 2961.
12. Yang, H. H.; Han, C. D.; Ma, C. Y. J Appl Polym Sci 1985, 30, 3297.
13. Lee, C. H.; Lee, K. J.; Jeong, H. G.; Kim, S. W. Adv Polym Technol 2000, 19, 97.
14. Brennecke, J. F. Nature 1997, 389, 333.
15. Blanchard, L. A.; Hancu, D.; Beckman, E. J.; Brennecke, J. F. Nature 1999, 399, 28.
16. Sarbu, T.; Styranec, T.; Beckman, E. J. Nature 2000, 405, 165.
17. Leitner, W. Nature 2000, 405, 129.
18. Garcia-Leiner, M.; Song, J.; Lesser, A. J. J Polym Sci Part B: Polym Phys 2003, 41, 1375.
19. Shieh, Y.; Su, J.; Manivannan, G.; Lee, P. H. C.; Sawan, S. P.; Spall, W. D. J Appl Polym Sci 1996, 59, 695.
20. Shieh, Y.; Su, J.; Manivannan, G.; Lee, P. H. C.; Sawan, S. P.; Spall, W. D. J Appl Polym Sci 1996, 59, 707.
21. Cooper, A. I.; Londono, J. D.; Wignall, G.; McClain, J. B.; Samulski, E. T.; Lin, J. S.; Dobrynin, A.; Rubinstein, M.; Burke, A. L. C.; Fréchet, J. M.; DeSimone, J. M. Nature 1997, 389, 368.
22. Zachariades, A. E.; Porter, R. S. J Appl Polym Sci 1979, 24, 1371.
23. Garcia-Leiner, M.; Lesser, A. J. In: Proceedings of ANTEC, Society of Plastics Engineers, San Francisco, CA, 2002.
24. Drobny, J. G. Technology of Fluoropolymers; CRC Press: Boca Raton, FL, 2000.
25. Chow, T. S. Macromolecules 1980, 13, 362.
26. Royer, J. R.; DeSimone, J. M.; Kahn, S. A. J Polym Sci Part B: Polym Phys 2001, 39, 3055.
27. Tervoort, T.; Visjager, J.; Graf, B.; Smith, P. Macromolecules 2000, 33, 6460.
28. Rajagopalan, P.; McCarthy, T. J. Macromolecules 1998, 31, 4791.
29. Lau, S. F.; Wesson, J. P.; Wunderlich, B. Macromolecules 1984, 17, 1102.
30. Lau, S. F.; Suzuki, H.; Wunderlich, B. J Polym Sci Polym Phys Ed 1984, 22, 379.
31. Arora, K. A.; Lesser, A. J.; McCarthy, T. J. Macromolecules 1999, 32, 2562.
32. Wunderlich, B. J Phys Chem 1960, 64, 1052.
33. Gaur, U.; Wunderlich, B. Polym Prepr (Am Chem Soc Div Polym Chem) 1979, 20, 429.
34. Pasztor, A. J.; Landes, B. J.; Karjala, P. J. Thermochim Acta 1991, 177, 187.
35. Arora, K. A.; Lesser, A. J.; McCarthy, T. J. Macromolecules 1998, 31, 4614.
36. Handa, Y. P.; Zhang, Z.; Wong, B. Macromolecules 1997, 30, 8499.
37. Handa, Y. P.; Zhang, Z. Macromolecules 1997, 30, 8505.